ISSN 1948-9358 (online)

World Journal of *Diabetes*

World J Diabetes 2018 December 15; 9(12): 206-257

Published by Baishideng Publishing Group Inc

World Journal of Diabetes

Contents

Monthly Volume 9 Number 12 December 15, 2018

NAME OF JOURNAL
World Journal of Diabetes

ISSN
ISSN 1948-9358 (online)

LAUNCH DATE
June 15, 2010

FREQUENCY
Monthly

EDITORIAL OFFICE
Jin-Lei Wang, Director
World Journal of Diabetes
Baishideng Publishing Group Inc
7901 Stoneridge Drive, Suite 501,
Pleasanton, CA 94588, USA
Telephone: +1-925-2238242
Fax: +1-925-2238243
E-mail: editorialoffice@wjgnet.com
Help Desk: https://www.f6publishing.com/helpdesk
https://www.wjgnet.com

PUBLISHER
Baishideng Publishing Group Inc
7901 Stoneridge Drive, Suite 501,
Pleasanton, CA 94588, USA
Telephone: +1-925-2238242
Fax: +1-925-2238243
E-mail: bpgoffice@wjgnet.com
Help Desk: https://www.f6publishing.com/helpdesk
https://www.wjgnet.com

PUBLICATION DATE
December 15, 2018

INSTRUCTIONS TO AUTHORS
https://www.wjgnet.com/bpg/gerinfo/204

ONLINE SUBMISSION
https://www.f6publishing.com

World Journal of Diabetes

Submit a Manuscript: https://www.f6publishing.com

World J Diabetes 2018 December 15; 9(12): 239-251

DOI: 10.4239/wjd.v9.i12.239

ISSN 1948-9358 (online)

ORIGINAL ARTICLE

Basic Study

Pathological changes in the cellular structures of retina and choroidea in the early stages of alloxan-induced diabetes

Irina Danilova, Svetlana Medvedeva, Svetlana Shmakova, Margarita Chereshneva, Alexey Sarapultsev, Petr Sarapultsev

Irina Danilova, Svetlana Medvedeva, Svetlana Shmakova, Department of Biology and Fundamental Medicine, Institute of Natural Sciences and Mathematics, Ural Federal University Named After the First Pres. of Russia B.N. Yeltsin, Ekaterinburg 620002, Russia

Irina Danilova, Svetlana Medvedeva, Svetlana Shmakova, Laboratory of Morphology and Biochemistry, Institute of Immunology and Physiology, Ural Division of Russian Academy of Sciences, Ekaterinburg 620049, Russia

Margarita Chereshneva, Laboratory of Immunophysiology and Immunopharmacology, Institute of Immunology and Physiology, Ural Division of Russian Academy of Sciences, Ekaterinburg 620049, Russia

Alexey Sarapultsev, Petr Sarapultsev, Institute of Chemical Engineering, Ural Federal University Named After the First Pres. of Russia B.N. Yeltsin, Ekaterinburg 620002, Russia

Alexey Sarapultsev, Petr Sarapultsev, Laboratory of Immunophatophysiology, Institute of Immunology and Physiology, Ural Division of Russian Academy of Sciences, Ekaterinburg 620049, Russia

ORCID number: Irina Danilova (0000-0001-6841-1197); Svetlana Medvedeva (0000-0002-0691-7579); Svetlana Shmakova (0000-0002-6552-7327); Margarita Chereshneva (0000-0002-6169-7978); Alexey Sarapultsev (0000-0003-3101-9655); Petr Sarapultsev (0000-0002-4093-4380).

Author contributions: Danilova I, Chereshneva M, Sarapultsev P, and Sarapultsev A contributed to the conception of the manuscript, design of experiments, and analysis and interpretation of the data, and wrote the manuscript; Danilova I, Medvedeva S, Shmakova S, and Sarapultsev A performed the experiments, analyzed the data, and wrote the manuscript; all authors have commented on the initial and final drafts of the manuscript and are responsible for approval of the final version of the manuscript in all aspects.

Supported by the Russian Science Foundation, No. 16-15-00039.

Institutional review board statement: This study protocol was reviewed and approved by the Institutional Review Board of Institute of Immunology and Physiology of Ural Branch of RAS, Ekaterinburg, Russia.

Institutional animal care and use committee statement: All institutional and national guidelines for the care and use of laboratory animals were followed. All experimental procedures with the animals were approved by the Institute of Animal Care and Use Committee at the Institute of Immunology and Physiology of the Ural Division of RAS (diab-1-04-2016).

Conflict-of-interest statement: The authors declare that there is no conflict of interest regarding the publication of this paper.

ARRIVE guidelines statement: The authors have read the ARRIVE guidelines, and the manuscript was prepared and revised according to the ARRIVE guidelines.

Manuscript source: Unsolicited manuscript

Corresponding author to: Alexey Sarapultsev, MD, PhD, Senior Researcher, Laboratory of Immunophatophysiology, Institute of Immunology and Physiology, Ural Division of Russian Academy of Sciences, 106 Pervomayskaya Street, Ekaterinburg 620049, Russia. a.sarapultsev@gmail.com
Telephone: +7-343-3740070
Fax: +7-343-3740070

Received: June 26, 2018
Peer-review started: June 26, 2018
First decision: July 19, 2018
Revised: September 1, 2018
Accepted: November 2, 2018
Article in press: November 3, 2018
Published online: December 15, 2018

Abstract

AIM

To investigate the temporal sequence of pathological changes in the cellular structures of retina and choroidea in the early stages of diabetes in laboratory animals.

METHODS

Experimental type 1 diabetes was modeled by three intraperitoneal injections of an alloxan solution into 30 male nonlinear rats at 16 wk of age. The 30th and 60th days from the final alloxan injection were chosen as the endpoints. Light and electron microscopy and morphometric and immunohistochemical studies were performed on histological slices of eyeballs from experimental animals.

RESULTS

Diabetic disturbances progressed to 60 d of the experiment. Thus, in the retina, a partial destruction of photoreceptors accompanied by interstitial edema was observed. The morphometric analysis revealed a reduction in the thickness of the retina. A reduction in the number of blood vessels of the choroid with disturbances of the endothelial cells and the vascular walls and a persistent reduction in the number of melanocytes were observed. The number of proliferating Ki-67 positive cells decreased, and the number of macrophages increased with diabetes development.

CONCLUSION

The starting point in the development of destructive changes involves early reduction in the number of melanocytes of the choroidea and alterations in the retinal pigment epithelium.

Key words: Alloxan; Diabetes; Diabetic retinopathy; Early stage; Morphology; Histological changes

Core tip: Diabetic retinopathy is the most frequent microvascular complication of diabetes. However, most of therapeutic approaches being developed do not address the early and potentially reversible failure of retinal perfusion. Thus, we examined pathological changes in the cellular structures of retina and choroidea in the early stages of diabetes in laboratory animals. According to the obtained results, the starting point in the development of destructive changes involves the early reduction in the number of melanocytes of the choroidea and the destruction of the retinal pigment epithelium, accompanied by an inflammatory process, which may represent a potential therapeutic target.

Danilova I, Medvedeva S, Shmakova S, Chereshneva M, Sarapultsev A, Sarapultsev P. Pathological changes in the cellular structures of retina and choroidea in the early stages of alloxan-induced diabetes. *World J Diabetes* 2018; 9(12): 239-251
URL: https://www.wjgnet.com/1948-9358/full/v9/i12/239.htm
DOI: https://dx.doi.org/10.4239/wjd.v9.i12.239

INTRODUCTION

Diabetic retinopathy (DR) is one of the major complications associated with diabetes, and has equally been implicated as one of the leading causes of visual impairment and blindness globally. Because of this, DR is in the limelight of most clinical studies[1-4]. Hyperglycemia, hypertension, renal disease, and dyslipidemia, which are typical conditions in the manifestation of diabetes, have all been linked to the pathogenesis of DR[5,6]. According to the prevailing point of view, the leading causes of DR development include metabolic disturbances and vascular bed abnormalities, which accompany diabetes development[7-11]. In diabetes, hyperglycemia and associated oxidative stress trigger the pathological cascade underlying the vascular injury (micro- and macroangiopathy development)[12-14]. Due to the subsequent disturbances of vessel walls, the permeability of the hematoretinal barrier breaks down, and hypoxia appears, leading to trophic retinal degeneration and photoreceptor cell death[15-17]. The subsequent progression of the developed retinopathy leads to retinal neovascularization, vitreous hemorrhages, and the formation of fibrous tissue in the foci of preretinal hemorrhages, which forms the pathogenomic picture of diabetic complications[18-20].

However, despite the seeming transparency of DR pathogenesis and the progress in its treatment observed in recent years, a number of issues remain that warrant further study[6,21-23]. One of them is the temporal sequence of pathological changes in DR development[19-22]. Studies in rodents have highlighted that biomarkers of inflammation, such as leukostasis, overexpression of adhesion molecules in retinal vascular endothelial cells and leukocytes, vascular permeability alteration, and aggrevated production of nitric oxide, prostaglandins, cytokines, and other inflammatory mediators appears in the retina during 1-6 mo of diabetes crisis[5]. Most developed therapies for DR, have primarily focused on the terminal stage of this disease, and as thus, failed to address the early potentially reversible stage of this disease. In addition, most of

Table 1 Level of glucose and glycosylated hemoglobin in the blood of experimental animals (mmol/L)

Biochemical parameters	Control animals (Group 1)	Diabetes, 30 d (2nd group)	Diabetes, 60 d (2nd group)
Glucose (mmol/L)	5.99 ± 0.33	25.98 ± 1.84[a]	32.60 ± 0.80[a]
Hb A1c (%)	5.12 ± 0.24	7.10 ± 0.60[a]	6.45 ± 0.29[a]
Insulin (μg/L)	1.28 ± 0.19	0.47 ± 0.05[a]	0.36 ± 0.04[a]

[a]Differences to control animals were significant at $P < 0.05$.

these therapies have been associated with severe sight-threatening side effects[6].

With that, understanding of the temporal sequence and stages of pathological disturbances of DR development is of great prognostic and scientific value, as it might contribute to improvements to current methods or even the development of new methods of diagnosis and treatment of such a serious complication of diabetes. Thus, this work investigated the temporal sequence of pathological changes in the cellular structures of retina and choroidea in the early stages of diabetes in laboratory animals.

MATERIALS AND METHODS

Animal preparation

Healthy, sexually matured male Wister rats were used for the purpose of this experiment. The animals employed in this study were quarantined in the vivarium of the Institute of Immunology and Physiology of the Ural Division of RAS (Ekaterinburg, Russia). Only animals showing no symptoms of any disease were selected. All experimental animals were housed in similar conditions, and fed according to a customary schedule. All the experimental procedures conducted on the animals were approved by the Institute of Animal Care and Use Committee at the Institute of Immunology and Physiology of the Ural Division of RAS (diab-1-04-2016), and implemented in compliance with the principles formulated in the European Convention for the Protection of Vertebrate Animals used for Experimental and Other Scientific Purposes (Strasbourg, France, 18.03.1986), APS's Guiding Principles in the Care and Use of Vertebrate Animals in Research and Training, and the Laboratory Practice Regulations of Russia Federation (Ministry of Public Health Order No. 267 from 19.06.2003).

Experimental model of type 1 diabetes

Experimental type 1 diabetes was modeled by three intraperitoneal injections (10 mg/100 g of weight) of an alloxan solution (Sigma-Aldrich, St. Louis, MO, United States) dissolved in physiological saline at 1 d intervals (total dose of alloxan 30 mg/100 g) according to a modified version of the standard model of diabetes in rats[24,25]. Alloxan is a toxic glucose analogue that has been employed to induce experimental diabetes. This compound accumulates in pancreatic cells and selectively destroys the insulin producing beta-cells[26,27].

Experimental protocol

The experiments were conducted on 30 male nonlinear rats of the same age (16-wk-old). The 30th and 60th days from the final alloxan injection were chosen as the endpoints of the experiment. This duration of diabetes in rats corresponds to a duration of diabetes in humans approximately equal to 4.25 and 8.5 years, which is a sufficient time for the development of diabetes complications, including neurodegenerative complications[17,28]. Thirty rats with body weight of 190-220 g were randomly divided into three groups (n = 10 in each group): control (group 1), diabetes 30 d (group 2), and diabetes 60 d (group 3). The control animals (group 1) received *i.p.* saline injections at day 1 and between 30-60 d (20 injections in total). The diabetes 30 d animals(group 2), weighing approximately 207 ± 10 g, were rendered diabetic after 16 h fasting conditions, by a single *i.p.* administration of alloxan monohydrate (Sigma-Aldrich, St. Louis, MO, United States) at a dose of 300 mg/kg of body weight, dissolved in 10 mmol/L of sodium citrate (pH 4.5). Afterwards, the animals were housed in standard conditions until the end of the 30 d experimental duration of the group. The diabetes 60 d animals (group 3), weighing 207 ± 10 g, received a single *i.p.* dose of 300 mg/kg alloxan monohydrate and were housed in similar conditions for 60 d. Peripheral blood glucose from the tail vein was obtained to determine glycemia in all experimental groups (Table 1).

On the respective sacrifice dates of each animal, they were first anaesthetized with 40 mg/kg pentobarbital sodium administered intraperitoneally. Blood samples (approximately 3 mL) were collected by heart puncture for biochemical and enzyme immunoassay investigations. Histological, immunohistochemical, and light and electron microscopy methods were used to study the rat's eye slices.

Laboratory blood tests

Plasma glucose levels were determined with a standard glucose oxidase test kit (Novogluk-R, "VektorBest", Russia)[29,30]. The plasma insulin level was determined using a standard ELISA Rat assay (Insulin ELISA, Mercodia AB, Switzerland). Biochemical testing was carried out with a DU-800 spectrophotometer (Beckman Coulter Int S.A., Switzerland).

HbA1c measurement was performed by affinity chromatography ("Diabetes-test", (HbA1c) TOR 9398240-16404416-01, Fosfosorb OJSC, Russian Federation), according to the manufacturer's instructions ("Fosfosorb" OJSC, Russia)[31].

Histological studies

A neutral buffered solution of 10% formalin was used to preserve the eye samples for 24 h, then paraffinized through a series of solutions[30]. The standard dehydration procedure was performed. The tissue was processed and embedded in paraffin wax using the autoprocessor Leica EG 1160. Hematoxylin and eosin (HE) staining of the 3-5 micron thick sections were performed for morphological and morphometric studies. The remaining sections were placed in a buffer for antigen unmasking and further immunohistochemical studies.

Immunohistochemical studies

For immunohistochemical evaluation, tissues were first fixed in formalin, then embedded in paraffin, and sectioned at 3 μm. The antibody staining of the tissues was performed with the Autostainer DAKO, according to a standard protocol. High-temperature treatment in a citrate buffer (pH = 6) using Pascal DAKO[32-34], was employed for the unmasking procedure of antigens. The visualization of antigen-reactive cells was performed using the NovolinkTM Polymer Detection System (Novocastra Lab., Ltd), with its buffer solution consisting of a chromogenic agent 3.3-diaminobenzidine (DAB). Macrophages were visualized with anti-CD68 antibodies (clone KP1, Thermo Scientific). The assessment of proliferation was performed with mouse anti-rat monoclonal antibodies to the Ki-67 marker (clone MM1, Leica Microsystems).

Morphometric analysis

Using sections of eyeballs stained with HE, the number of vessels and melanocytes per unit area (0.01 mm^2 tissue of choroid) (N/0.01 mm^2) was estimated in the choroidea, whereas the total thickness and the thickness of separate layers (in μm) were estimated in the retina.

The number of proliferating cells in the ganglionic and internal nuclear retinal layers was estimated on sections stained with the Ki-67 proliferation marker, the ratio of the total proliferating cells to total number of cells in the retina layer was subsequently calculated. Using sections stained with CD68 marker, the number of CD68 positive cells per unit area (1 mm^2 tissue) (N/mm^2) was determined in the choroidea and the retina.

Optical-microscopic examination

Optical-microscopic examination was conducted with the microscope (Leica DM 2500), and the analysis of the image was done using Video TesT "Morphology" 5.0 program (VideoTesT, St. Petersburg, Russia).

Electron microscopy examination

For ultramicroscopic examination after enucleation of the eyeball, the lens of the eye and the posterior wall of the eyeball containing the retina and the choroid were fixed in a 2.5% solution of glutaraldehyde followed by postfixation in a 1% solution of osmium tetroxide (OsO4). After thorough washing, dehydration in alcohols of increasing concentrations (50%, 70%, 96% and 100%) was performed followed polymerization in an araldite resin at a temperature of 60 ℃[35]. Slices were created using ultramicrotome (Leica EM UC6), contrasted with lead citrate, and examined with the aid of a digital transmission electron microscope (Morgagni™ 268).

Statistical analysis

Analysis of data was performed using Statistica 6.0 software (StatSoft, United States), variables showing results with a heterogeneous distribution were analyzed using the nonparametric (*U*) Mann-Whitney test. All analysis was carried out at 0.05% significance level of probability.

RESULTS

Confirmation of diabetes development

The development of diabetes in experimental animals was confirmed by biochemical study. According to the results, a significant increase in the levels of glucose and glycosylated hemoglobin (HbA1c) and a decrease in the level of insulin were detected after alloxan administration in the animals of experimental groups 2 and 3 compared to the control group (Table 1).

Experimental diabetes: Thirty days

Retina: Histological examination of the retina and choroid of animals in the control group exhibited no structural disturbances (Figures 1 and 2A). However, in experimental group 2, moderately pronounced interstitial edema and fullness of dome capillaries in the ganglionic and inner nuclear layers of the retina were observed (Figure 3A).

Electron microscopic examination confirmed the presence of edema in the form of an expansion of the spaces between the layers of rods and cones and their partial deformation and disorganization of the outer and inner segments of the photoreceptors (Figures 3B and 4). In the outer nuclear layer, round-shaped nuclei with irregular intervals between them were observed. This feature was attributed to the developing interstitial edema. The contours of the nuclei were even. The chromatin was osmiophilic in the center of the nucleus and bright on the periphery. The monolayer of cells

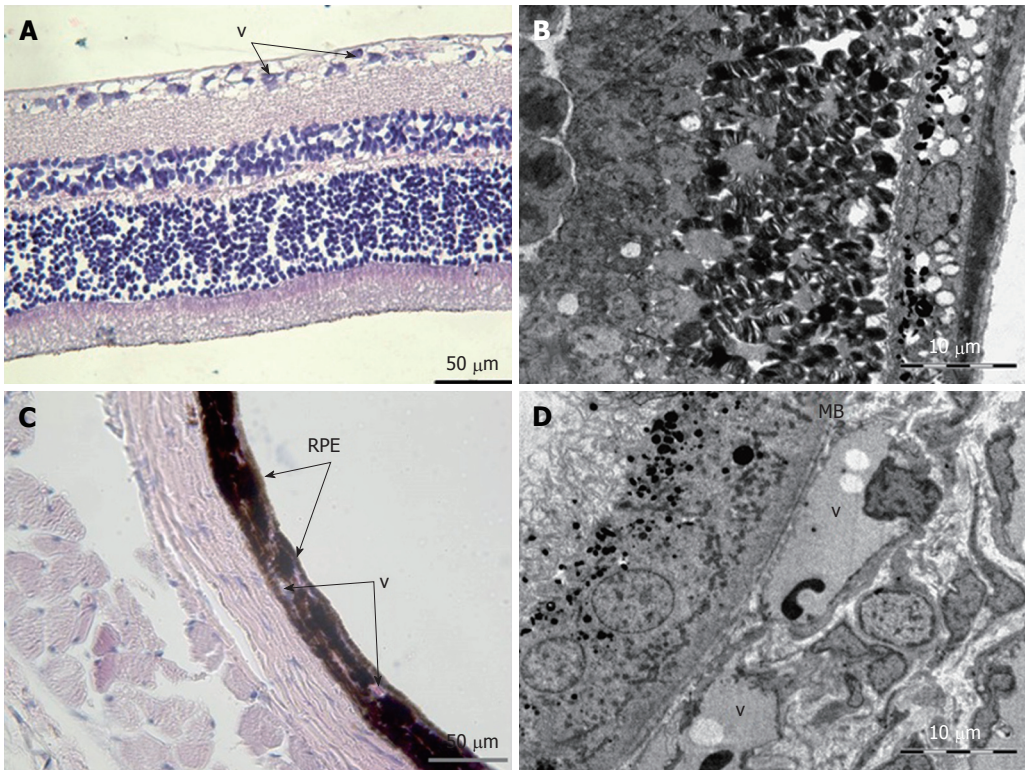

Figure 1 Back of the eye of a control animal. A: Light microscopy visualization of the retina. v: blood vessels; B: Electron microscopy of the outer layers of the retina; C: Light microscopy of the choroid and sclera of the eye. v: choroid vessels; RPE: pigment epithelium of the retina; D: Electron microscopy of the retinal pigment epithelium and choroid. v: choroid vessels; Light microscopy: staining with hematoxylin and eosin, magnification × 400, bar 50 μm; Electron microscopy: bar 10 μm.

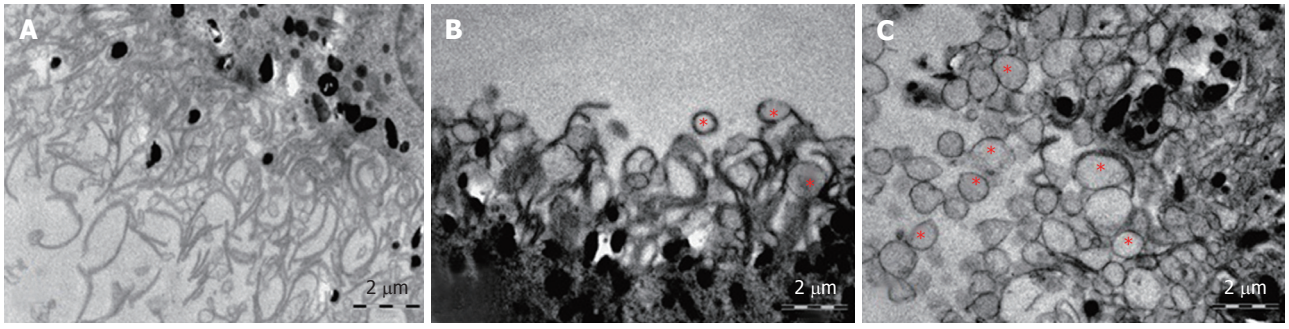

Figure 2 Cell processes of retinal pigment epithelium. A: Control animals (group 1); B: Diabetes at 30 d (group 2); C: Diabetes at 60 d (group 3); Bar 2 μm. *: vacuolation of cell processes.

of retinal pigment epithelium adhered to the Bruch's membrane. In the cytoplasm of the pigment epithelium, an uneven distribution with a quantitative decrease of pigment granules was detected (Figure 2B). Electron microscopy revealed loosening of the membranes of the pigment epithelium nuclei, mitochondrial swelling, the destruction of the crista, and the enlightenment of the mitochondrial matrix (Figure 3D).

Morphometric examination of the retina revealed changes in the thickness of different layers. Thus, a decrease in the total thickness of the retina and in the rods and cones, outer nuclear and ganglionic layers was revealed, indicating the development of dystrophic processes during the time course of diabetes (Table 2).

Choroidea: Morphometric analysis of the choroidea revealed a decrease in the number of blood vessels per unit area in group 2 (1.79 ± 0.07) compared to the control animals (2.62 ± 0.33) (Table 3, Figures 5 and 6).

According to the results of optical microscopic examination, alterations of the microcirculatory vessels in the choroidea were detected accompanied by desquamation and swelling of endothelial cells. These features led to the occlusion of small capillaries, the expansion of their limen, and the development of edema (Figure 2C).

Electron microscopic examination revealed a pro-

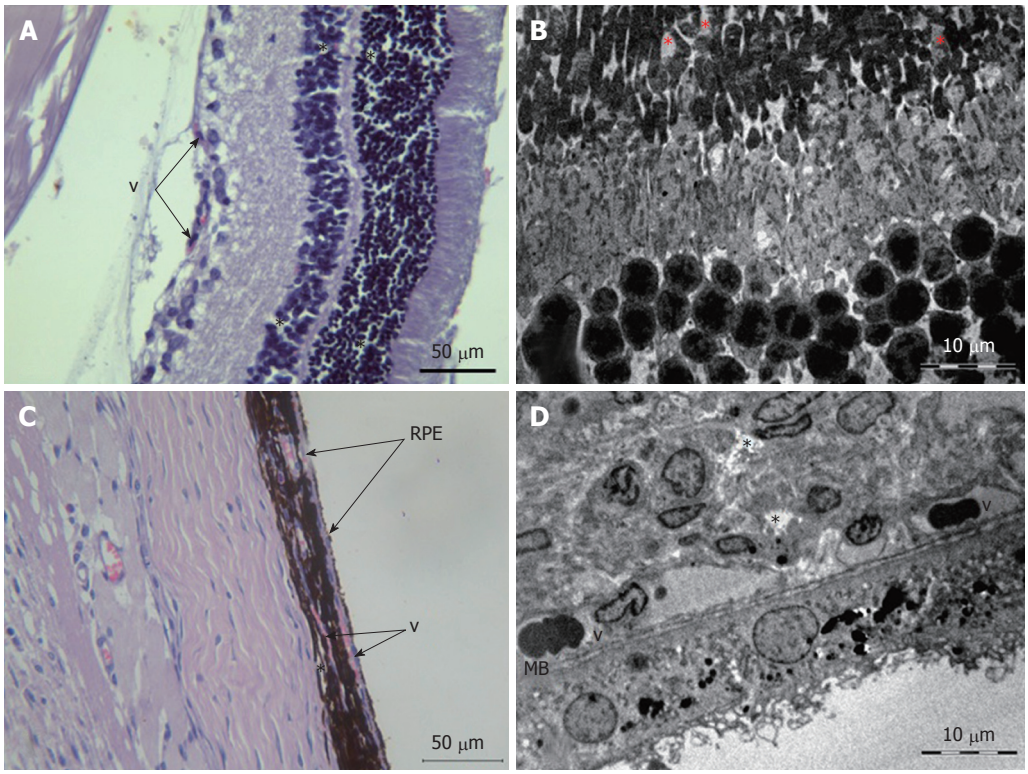

Figure 3 Posterior wall of the eye of an animal with diabetes at 30 d. A: Light microscopy of the retina; *: interstitial edema; v: full blood vessels; B: Electron microscopy of the outer layers of the retina; *: destroying rods and cones; C: Light microscopy of the choroid and sclera of the eye; *: interstitial edema; v: full blood vessels; RPE: destructive changes in retinal pigment epithelial cells; D: Electron microscopy of the retinal pigment epithelium and choroid; *: interstitial edema; v: choroid vessels with sludge complexes; MB: unevenly thickened Bruch's membrane; Light microscopy: staining with hematoxylin and eosin, magnification × 400, bar 50 μm; Electron microscopy: bar 10 μm.

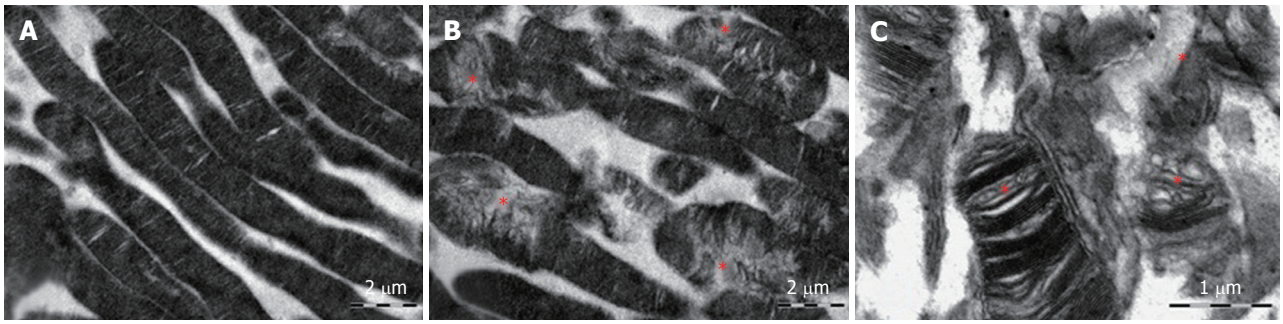

Figure 4 Photoreceptors of the retina. A: control animals (group 1), bar 2 μm; B: diabetes at 30 d (group 2), bar 2 μm; C: diabetes at 60 d (group 3), bar 1 μm. *: destruction of photoreceptors.

nounced loosening of the connective tissue with the formation of edema foci in the perivascular zone. The choroid was hypovascularized, and only a small number of vessels that were generally small in diameter were detected. In vessels, various alterations of the integrity of basal membranes as well as endothelial cell swelling and their partial destruction were clearly defined. The sluggish erythrocytes were visible in the lumen of capillaries (Figure 3D).

Based on light microscopy, the pigmented layer of the choroid after 30 d of experimental diabetes was characterized by pronounced dystrophic changes in melanocytes with the destruction of their cytoplasmic membrane and the release of pigment granules into the intercellular space.

According to the results of optical microscopic examination, the layer of melanocytes in the choroid was characterized by pronounced dystrophic changes in melanocytes with the destruction of their cytoplasmic membranes and signs of pigment granule release into the intercellular space. Melanocytes located perivascularly were characterized by the presence of pronounced dystrophic changes in their ultrastructure: the destruction of mitochondria and endoplasmic reticulum and the output of secretory granules to the extracellular space. The number of choroidal melanocytes was significantly

Table 2 Characteristics of the thickness of the retina and its individual layers (μm, M ± m)

Group	Retinal layers						Total thickness of the retina
	Layer rods and cones	Outer nuclear layer	Outer plexiform layer	Inner nuclear layer	Inner plexiform layer	Ganglion cell layer	
Control (group 1)	36.31 ± 5.11	56.43 ± 1.72	9.85 ± 1.68	25.82 ± 0.76	38.93 ± 4.79	17.82 ± 0.72	185.16 ± 9.42
Diabetes at 30 d (group 2)	28.65 ± 3.44[a]	51.62 ± 6.51[a]	11.46 ± 1.59	26.1 ± 1.55	40.21 ± 7.14	15.98 ± 1.37[a]	174.00 ± 2.93[a]
Diabetes at 60 d (group 3)	28.38 ± 1.43[a]	56.87 ± 5.30	9.69 ± 1.04[c]	26.24 ± 0.95[a]	39.94 ± 7.10	14.65 ± 2.05[a]	175.77 ± 5.22[a]

[a]Differences compared to control animals were significant at $P < 0.05$; [c]Differences compared to animals with diabetes at 30 d were significant at $P < 0.05$.

reduced per unit area (20.5 ± 0.39) compared to the control animals (10.1 ± 2.42) (Table 4).

Immunohistochemical study results: Proliferating cells are localized in the inner nuclear and ganglionic layers or retina, where glia cells capable of proliferating are present. Ki-67 positive cells were reduced in the inner nuclear and ganglionic layers of the retina in both the absolute and relative indices, and the decrease was more pronounced in the ganglionic layer (Table 4, Figures 7 and 8).

Immunohistochemical staining of the choroid and retina with anti-CD68 antibodies revealed a decrease in the number of macrophages in the retina, both in the ganglionic and inner nuclear layers compared to control animals. No significant changes were observed in the choroidea (Table 5).

Experimental diabetes: Sixty days

Retina: Histological examination of the retina of experimental animals from group 3 revealed an increase in dystrophic changes of photoreceptor and pigment epithelium layers compared to the histological features of group 2 animals (Figure 4). A plethora of capillaries of the retinal ganglionic layer and foci of angiomatosis in the inner nuclear layer were also observed (Figure 9).

Morphometric examination of the retina revealed changes in the thickness of different layers. Thus, a decrease in the thickness of the photoreceptor layer, internal nuclear, ganglionic, and outer reticular layers was revealed, indicating the dynamics of the development of dystrophic processes during the time course of diabetes (Table 2 and Figure 6).

Electron microscopic examination revealed signs of partial destruction of the layer of rods and cones. The remains of the membrane discs were observed, some of which were clearly visualized. In the inner nuclear layer, small diameter vessels of the sinusoidal type were observed (Figure 9B). Cells of the pigment epithelium of the retina were arranged on Bruch's membrane, exhibiting a folded, uneven shape with invagination sites (Figure 2C). The nuclei of the pigment cells and pigment granules were determined extracellularly, and cell outgrowths were in a state of destruction (Figure 9D).

Choroidea: Melanocyte dystrophy (a redistribution of melanin granules with a decrease in the total number of cells), which was described in group 2, was preserved (Table 3 and Figure 9C).

In the connective tissue layer, focal vascular fullness with the formation of sludge complexes was revealed and accompanied by the occlusion of some vessels, endothelial cell swelling, and the destruction of the basal membrane. The number of vessels per unit area corresponded to the values obtained at 30 d (Table 3).

Electron microscopy examination revealed loosening of connective tissue and massive perivascular edema. Most of the observed vessels were characterized by an enlarged lumen with swollen endothelial cells. The cytoplasmic membrane of the endothelial cells and their nuclei were uneven and folded. Swollen mitochondria with a visible matrix and the remnants of crista were detected inside the cells.

Results of immunohistochemical study: The immunohistochemical study of Ki-67 positive cells revealed that their quantity did not decrease and were similar to group 2 (Table 4, Figures 7 and 8).

Table 3 Average number of blood vessels and pigment cells in the choroid of the eyes of experimental animals (per unit area, S = 0.01 mm^2)

	Control (group 1)	Diabetes at 30 d (group 2)	Diabetes at 60 d (group 3)
No. of blood vessels	2.62 ± 0.33	1.79 ± 0.07[a]	1.59 ± 0.22[a]
No. of pigment cells	35.23 ± 5.69	20.5 ± 0.39[a]	10.1 ± 2.42[a]

[a]Differences compared to control animals were significant at $P < 0.05$.

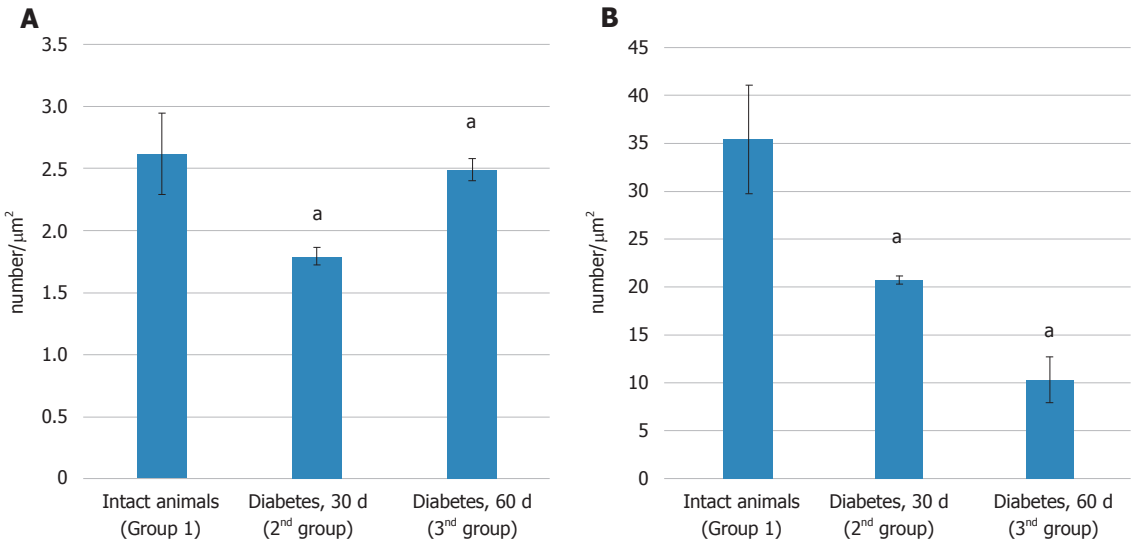

Figure 5 Morphometric examination of the choroid of the eyes of animals in experimental groups. A: The average number of choroidal vessels per unit area (0.01 mm^2); B: Average number of pigment cells of the choroid per unit area (0.01 mm^2). [a]Differences compared to the control animals were significant at $P < 0.05$.

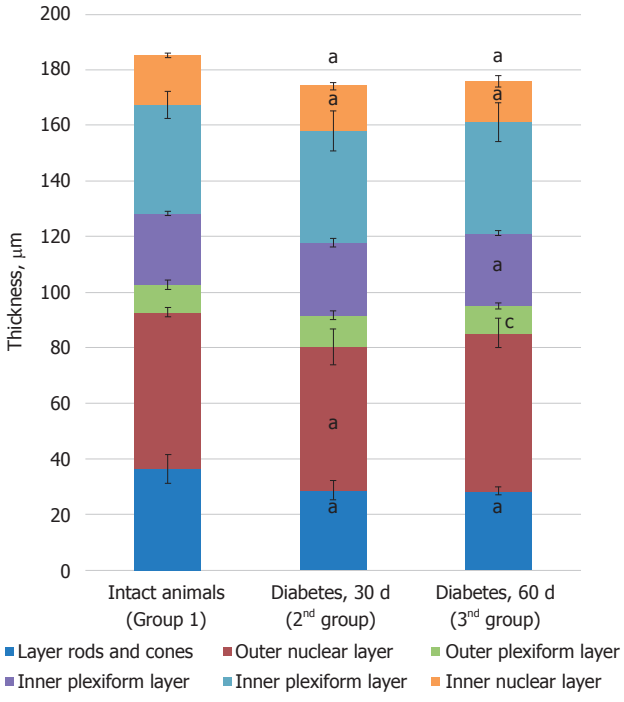

Figure 6 Morphometric examination of retinal layers of experimental groups. [a]Differences compared to control animals were significant at $P < 0.05$; [c]Differences to animals with diabetes for 30 d were significant at $P < 0.05$.

Immunohistochemical staining of the choroidea and retina with anti-CD68 antibodies revealed an increase in the number of macrophages in choroidea compared to group 1 and group 2. The quantity of macrophages in the inner layer of the retina was similar to group 2. In the ganglionic layer, an increase in the number of macrophage was equal to the control group (Table 5).

DISCUSSION

A plethora of evidence obtained over the past 20 years based on different clinical studies and experimental data have shed more light on the development and pathogenesis of DR and how it develops[6,10,11,36,37]. However, the complexity of pathogenic pathways that lead to the development of DR is beyond the scope of this article and are reviewed elsewhere[5,6,10,11,36]. The typical histological picture of diabetes characterized by the destruction of stroma and cell elements was also described in a number of studies[37].

The aim of the present study was to supplement this picture with the use of immunohistochemical and morphometric methods of investigation to estimate the numbers and proliferation status of individual cellular elements (melanocytes), thus providing information about the time course of destructive processes with the focus on the early stages of diabetes development.

In the present study, the alloxan-induced diabetes model demonstrated that in the early stages of the

Table 4 Number of Ki-67 positive cells in the layers of the retina (M ± m)

Group	Layers of the retina					
	Inner nuclear layer			Ganglion cell layer		
	1000 at 1 mm^2		% of Ki-67 positive cells	1000 at 1 mm^2		% of Ki-67 positive cells
	All cells	Ki-67 positive cells		All cells	Ki-67 positive cells	
Control (group 1)	28.60 ± 2.11	7.25 ± 0.93	25.46 ± 3.53	7.71 ± 1.01	0.99 ± 0.3	12.98 ± 3.24
Diabetes at 30 d (group 2)	27.94 ± 1.14	4.92 ± 0.92[a]	17.82 ± 3.79[a]	5.45 ± 0.78[a]	0.42 ± 0.18[a]	7.83 ± 3.11[a]
Diabetes at 60 d (group 3)	29.24 ± 2.56	4.55 ± 1.5[a]	15.4 ± 4.76[a]	6.19 ± 0.79[a]	0.59 ± 0.3[a]	9.95 ± 5.12

[a]Differences compared to control animals were significant at $P < 0.05$.

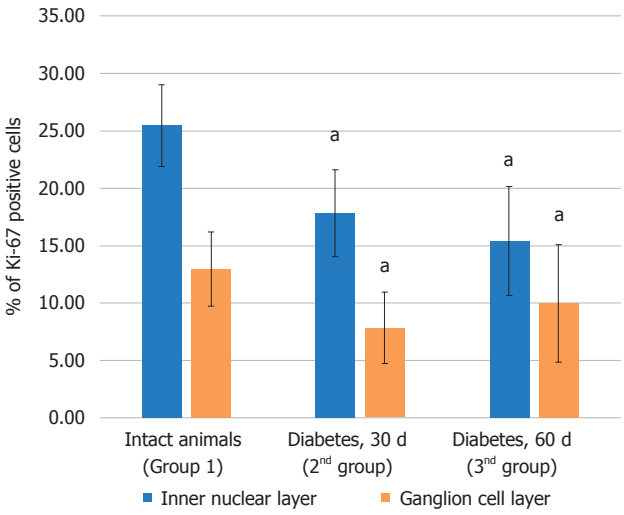

Figure 7 Relative content of Ki-67 positive cells from the total number of cells in the inner nuclear and ganglionic layers of the retina. [a]Differences compared to control animals were significant at $P < 0.05$.

disease (30 d), diabetic alterations in the structures of the retina and choroid are present, and these alterations progress slightly after 60 d.

In the retina, these disorders manifest themselves as a partial destruction of the structural-functional elements, namely, photoreceptors and are accompanied by a stromal reaction in the form of the development of interstitial edema, which was confirmed by the histological and electron microscope images of the examined structures[38]. In addition, morphometric analysis revealed a reduction in the thickness of the retina due to photoreceptor destruction. Moreover, in retinal layers that are capable of proliferation (the inner nuclear layer and ganglionic layer), the number of Ki-67 positive cells decreased with the development of diabetes.

The choroidea consists of a network of chorio-capillaries and stroma. Similar to other types of connective tissue, mast cells, macrophages, and lymphocytes are present in the stroma[39]. It is believed that the vascular membrane fulfills the function of supplying the outer layers of the retina with oxygen and nutrients. Thus, disruption of the choriocapillary structure causes degenerative changes in the latter and its neovascularization[39-41]. However, the precise cellular mechanisms leading to retinal dysfunction under high glucose levels remain unclear.

According to these results, a reduction in the number of blood vessels of the choroid with the pathological alterations of endothelial cells and vascular walls were observed. Moreover, the described changes develop during early stages of the disease (30 d) and generally do not change as time progresses.

Pathological changes in the number and state of cellular elements of the stroma of choroidea (melanocytes and macrophages) complete the picture of DR. Thus, the persistent reduction in the number of melanocytes in the choroidea (1.5-fold at 30 d and 3-fold at 60 d) was observed. Moreover, the pigment epithelium of the retina exhibited signs of dystrophic changes in the ultrastructure of cells accompanied by a reduction in the amount and redistribution of melatonin granules in these cells. Moreover, given that melanocytes release the key factors of angiogenesis, such as fibromodulin, a reduction in melanocytes may be one of the factors that leads to the above described reduction in the number of capillaries in the choroidea[42].

Macrophages are present in the choroidea under normal conditions, performing homeostatic functions[42]. However, in DR macrophages play a key role in the development of the inflammatory response, releasing pro-inflammatory cytokines that lead to capillary degeneration[43]. Moreover, according to Aveleira *et al*[44], the proapoptotic effect of inflammatory cytokines is significantly increased with hyperglycemia. According to our results, an increase in the number of macrophages (3.5-fold) in the choroidea was observed in diabetes[44]. Apparently, such a pronounced macrophage infiltration was caused by the recruitment of cells of the monocyte-macrophage lineage from the blood stream, as evidenced by their perivascular localization. The initiating factor of the observed migration of macrophages into the choroid was the development of destructive disorders (inflammation) in the latter[45].

Finally, a significant reduction (3.5-fold) in the number of pigment cells was also observed, which corresponds to findings reported in the literature[46]. This feature characterized the progression of pathological changes in the choroidea and led to further disruption of the integrity of the hematoretinal barrier[47].

In general, based on the results of our study, it can be assumed that the starting point in the development

Table 5 Quantitative distribution of macrophages in the eyes based on the structures (M ± m / 1 mm^2)

Structure of the eye		Control (group 1)	Diabetes at 30 d (group 2)	Diabetes at 60 d (group 3)
Choroidea		4.16 ± 3.31	4.99 ± 2.84	14.4 ± 6.69[a,c]
Retina	Ganglionic layer	18.46 ± 2.66	9.42 ± 1.00[a]	16.25 ± 5.30[c]
	Inner nuclear layer	11.25 ± 3.71	6.6 ± 2.59[a]	7.87 ± 1.71[a]

[a]Differences compared to control animals were significant at $P < 0.05$; [c]Differences compared to animals with diabetes at 30 d were significant at $P < 0.05$.

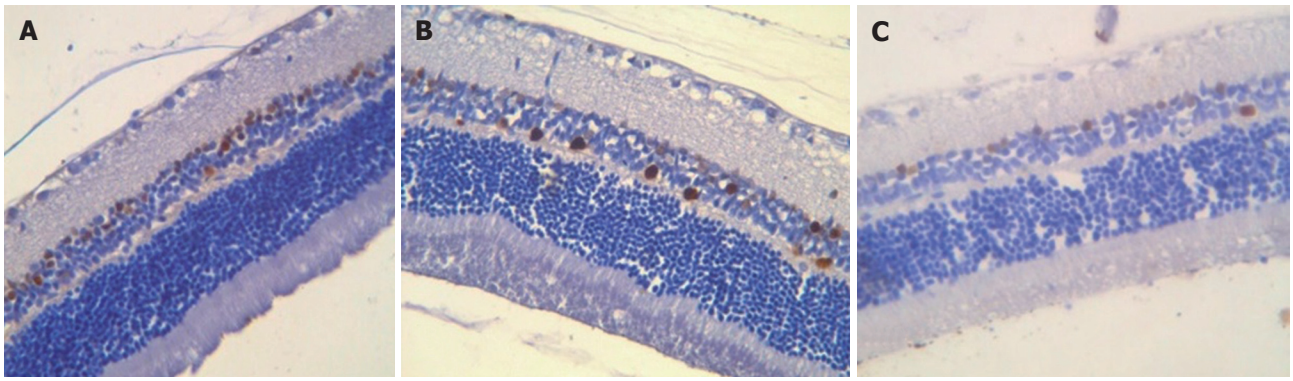

Figure 8 Ki-67 staining of the retina. A: Control animals; B: Diabetes at 30 d; C: Diabetes at 60 d.

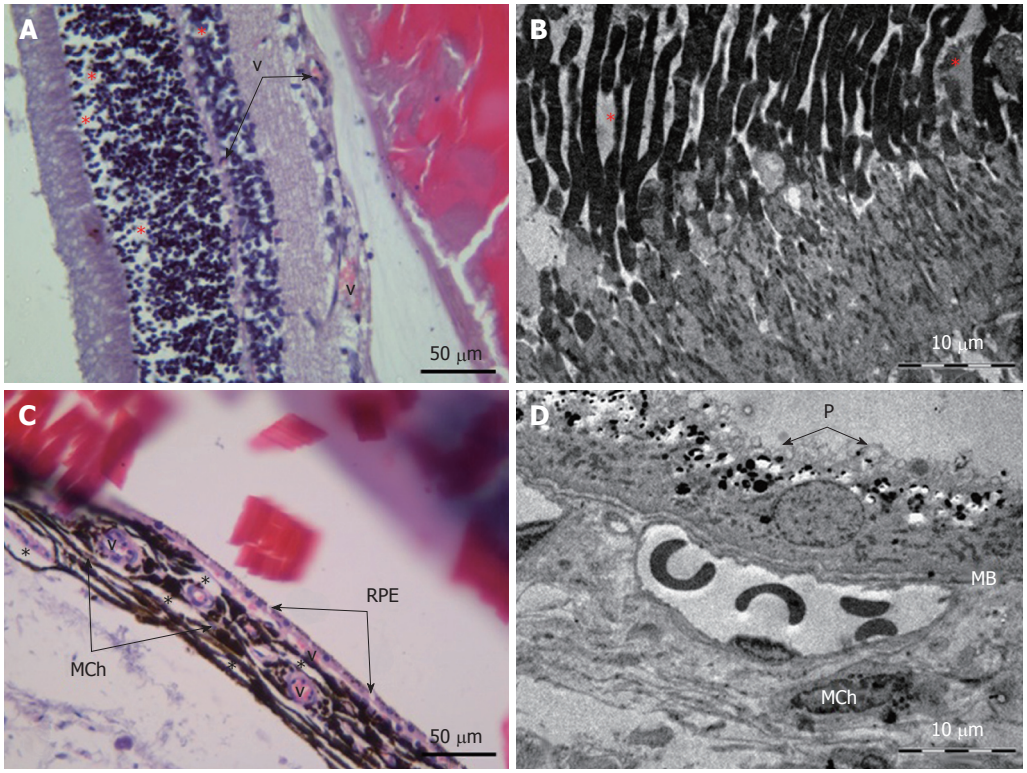

Figure 9 Posterior wall of the eye of an animal with diabetes at 60 d. A: Light microscopy of the retina; *: interstitial edema; v: full blood vessels; B: Electron microscopy of the outer layers of the retina; *: destruction of rods and cones; C: Light microscopy of the choroid of the eye; *: interstitial edema; v: full blood vessels with swollen endothelial cells; RPE: destructive changes in retinal pigment epithelial cells; MCh: destruction of pigment cells of the choroid; D: Electron microscopy of the retinal pigment epithelium and choroid; MB: uneven Bruch's membrane with invagination sites; MCh: choroidal melanocyte with reduced amount of pigment granules; P: destructive changes in the outgrowths of retinal pigment epithelial cells; Light microscopy: staining with hematoxylin and eosin, magnification × 400, bar 50 μm; Electron microscopy: bar 10 μm.

of destructive changes in DR involves the early reduction in the number of melanocytes of the choroidea and the destruction of the retinal pigment epithelium, which are the primary components of the hematoretinal barrier.

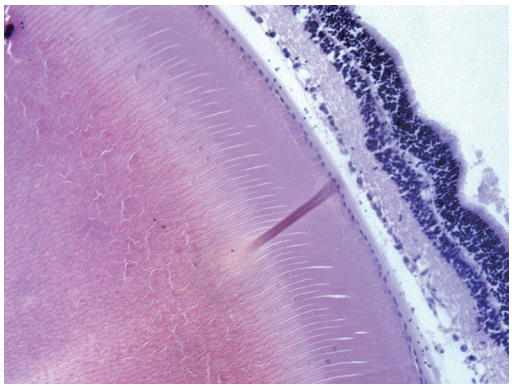

Figure 10 Fragment of the eye of an animal after alloxan administration at the dose of 30 mg/kg at 14 d. No visible structural changes are detected. Light microscopy: staining with hematoxylin and eosin, magnification × 400.

Limitations of the study

According to the literature, the direct toxic effects of alloxan on the retina, rather than secondary changes from diabetes, have been described[48-50]. Some teratogenic effects of alloxan in mice have been observed, including abnormalities of the lens and iris[49]. However, according to our results, the injection of alloxan in the total dose of 30 mg/100 g did not cause any disturbances at 14 d that could be observed via optical microscopy (Figure 10).

ARTICLE HIGHLIGHTS

Research background

Diabetic retinopathy (DR) is a disease commonly associated with diabetes complications. It is known as one of the primary causes of visual impairment and blindness globally. More recent discoveries have shown that indicators of inflammation, altered vascular permeability, and increased production of inflammatory mediators occurs in the retina after 1-6 mo of the presence of diabetes. However, most of therapeutic approaches being developed do not address the early and potentially reversible failure of retinal perfusion.

Research motivation

Better understanding of the temporal sequence and stages of pathological disturbances of DR development is of scientific value, as it might contribute to improvements to current methods or even the development of new methods of diagnosis and treatment of the early and potentially reversible failure of retinal perfusion.

Research objectives

We have investigated the temporal sequence of pathological changes in the cellular structures of retina and choroidea in a rat model of alloxan-induced diabetes in the early stages of disease.

Research methods

Alloxan accumulates in pancreatic cells, resulting in selective β-cell necrosis and diabetes. Experimental diabetes was modeled by three intraperitoneal injections (10 mg/100 g of weight) of an alloxan solution dissolved in physiological saline at 1-d intervals (total dose of alloxan 30 mg/100 g). The 30th and 60th days from the final alloxan injection were chosen as the endpoints of the experiment. Biochemical and enzyme immunoassay were performed. Furthermore, histological, immunohistochemical, and electron microscopy methods were employed to evaluate the rat's eye slices. Similarly, light microscopy and morphometric analyses of slides were also conducted.

Research results

In the present study, the alloxan-induced diabetes model demonstrated that in the early stages of the disease, diabetic alterations in the structures of the retina and choroid are present, and these alterations progress with time. In the retina, DR manifest itself as a partial destruction of the structural-functional elements, namely, photoreceptors and are accompanied by a stromal reaction in the form of the development of interstitial edema and a reduction in the thickness of the retina due to photoreceptor destruction. The reduction in the number of blood vessels of the choroid, melanocytes, and pigment cells along with an increase in the number of macrophages were also observed at early stages of the disease.

Research conclusions

The results of this study provide evidence that DR manifests itself at the early stages of diabetes. The starting point in the development of DR involves the early reduction in the number of melanocytes of the choroidea and the destruction of the retinal pigment epithelium, which are the primary components of the hematoretinal barrier.

Research perspectives

Further studies that estimated vascular endothelial growth factor, prostate-derived Ets transcription factor, cytokines, NO, and antioxidants and correlated them with blood glucose levels and changes in the retina in various experimental models and at different time periods will contribute to the improvements and the development of new methods of diagnosis and treatment of DR.

REFERENCES

1 **Constantino MI**, Molyneaux L, Wu T, Twigg SM, Wong J, Yue DK. Data collection on retinopathy as a public health tool: The Hubble telescope equivalent of looking back in time. *J Diabetes Complications* 2017; **31**: 721-725 [PMID: 28161385 DOI: 10.1016/j.jdiacomp.2016.12.016]

2 **Vujosevic S**, Pucci P, Casciano M, Daniele A, Bini S, Berton M, Cavarzeran F, Avogaro A, Lapolla A, Midena E. A decade-long telemedicine screening program for diabetic retinopathy in the north-east of Italy. *J Diabetes Complications* 2017; **31**: 1348-1353 [PMID: 28551296 DOI: 10.1016/j.jdiacomp.2017.04.010]

3 **Das A**. Diabetic retinopathy: Battling the global epidemic. *Indian J Ophthalmol* 2016; **64**: 2-3 [PMID: 26953017 DOI: 10.4103/0301-4738.178155]

4 **Yau JW**, Rogers SL, Kawasaki R, Lamoureux EL, Kowalski JW, Bek T, Chen SJ, Dekker JM, Fletcher A, Grauslund J, Haffner S, Hamman RF, Ikram MK, Kayama T, Klein BE, Klein R, Krishnaiah S, Mayurasakorn K, O'Hare JP, Orchard TJ, Porta M, Rema M, Roy MS, Sharma T, Shaw J, Taylor H, Tielsch JM, Varma R, Wang JJ, Wang N, West S, Xu L, Yasuda M, Zhang X, Mitchell P, Wong TY; Meta-Analysis for Eye Disease (META-EYE) Study Group. Global prevalence and major risk factors of diabetic retinopathy. *Diabetes Care* 2012; **35**: 556-564 [PMID: 22301125 DOI: 10.2337/dc11-1909]

5 **Chen M**, Stitt A. Animal Models of Diabetic Retinopathy. In: Chan CC, editor. Animal Models of Ophthalmic Diseases. Cham: Springer International Publishing, 2016: 67-83 [DOI: 10.1007/978-3-319-19434-9_5]

6 **Stitt AW**, Lois N, Medina RJ, Adamson P, Curtis TM. Advances in our understanding of diabetic retinopathy. *Clin Sci* (Lond) 2013; **125**: 1-17 [PMID: 23485060 DOI: 10.1042/CS20120588]

7 **Duță I**, Fica S, Ion DA. The Association between Insulin Resistance and Proliferative Retinopathy in Type 1 Diabetes. *Rom J Intern Med* 2015; **53**: 261-266 [PMID: 26710502 DOI: 10.1515/rjim-2015-0034]

8 **Kandarakis SA**, Piperi C, Topouzis F, Papavassiliou AG. Emerging role of advanced glycation-end products (AGEs) in the pathobiology of eye diseases. *Prog Retin Eye Res* 2014; **42**: 85-102 [PMID: 24905859 DOI: 10.1016/j.preteyeres.2014.05.002]

9 **Stem M**, Boynton G, Thompson A, Khan NW, Jackson GR, Pop-Busui R, Gardner TW. Inner retinal sensory neuropathy in persons with type 1 diabetes mellitus. *Invest Ophthalmol Vis Sci* 2014; **55**: 4426-4426

10 **Antonetti DA**, Klein R, Gardner TW. Diabetic retinopathy. *N Engl J Med* 2012; **366**: 1227-1239 [PMID: 22455417 DOI: 10.1056/NEJMra1005073]

11 **Kern TS**. Contributions of inflammatory processes to the development of the early stages of diabetic retinopathy. *Exp Diabetes Res* 2007; **2007**: 95103 [PMID: 18274606 DOI: 10.1155/2007/95103]

12 **Madsen-Bouterse SA**, Kowluru RA. Oxidative stress and diabetic retinopathy: pathophysiological mechanisms and treatment perspectives. *Rev Endocr Metab Disord* 2008; **9**: 315-327 [PMID: 18654858 DOI: 10.1007/s11154-008-9090-4]

13 **Barber AJ**, Lieth E, Khin SA, Antonetti DA, Buchanan AG, Gardner TW. Neural apoptosis in the retina during experimental and human diabetes. Early onset and effect of insulin. *J Clin Invest* 1998; **102**: 783-791 [PMID: 9710447 DOI: 10.1172/JCI2425]

14 **Roy S**, Kern TS, Song B, Stuebe C. Mechanistic Insights into Pathological Changes in the Diabetic Retina: Implications for Targeting Diabetic Retinopathy. *Am J Pathol* 2017; **187**: 9-19 [PMID: 27846381 DOI: 10.1016/j.ajpath.2016.08.022]

15 **Barber AJ**, Gardner TW, Abcouwer SF. The significance of vascular and neural apoptosis to the pathology of diabetic retinopathy. *Invest Ophthalmol Vis Sci* 2011; **52**: 1156-1163 [PMID: 21357409 DOI: 10.1167/iovs.10-6293]

16 **Barber AJ**. A new view of diabetic retinopathy: a neurodegenerative disease of the eye. *Prog Neuropsychopharmacol Biol Psychiatry* 2003; **27**: 283-290 [PMID: 12657367 DOI: 10.1016/S0278-5846(03)00023-X]

17 **Énzsöly A**, Szabó A, Kántor O, Dávid C, Szalay P, Szabó K, Szél Á, Németh J, Lukáts Á. Pathologic alterations of the outer retina in streptozotocin-induced diabetes. *Invest Ophthalmol Vis Sci* 2014; **55**: 3686-3699 [PMID: 24845643 DOI: 10.1167/iovs.13-13562]

18 **Zampetaki A**, Willeit P, Burr S, Yin X, Langley SR, Kiechl S, Klein R, Rossing P, Chaturvedi N, Mayr M. Angiogenic microRNAs Linked to Incidence and Progression of Diabetic Retinopathy in Type 1 Diabetes. *Diabetes* 2016; **65**: 216-227 [PMID: 26395742 DOI: 10.2337/db15-0389]

19 **Schorr SG**, Hammes HP, Müller UA, Abholz HH, Landgraf R, Bertram B. The Prevention and Treatment of Retinal Complications in Diabetes. *Dtsch Arztebl Int* 2016; **113**: 816-823 [PMID: 28073426 DOI: 10.3238/arztebl.2016.0816]

20 **Ford JA**, Lois N, Royle P, Clar C, Shyangdan D, Waugh N. Current treatments in diabetic macular oedema: systematic review and meta-analysis. *BMJ Open* 2013; **3**: pii: e002269 [PMID: 23457327 DOI: 10.1136/bmjopen-2012-002269]

21 **El Rami H**, Barham R, Sun JK, Silva PS. Evidence-Based Treatment of Diabetic Retinopathy. *Semin Ophthalmol* 2017; **32**: 67-74 [PMID: 27700224 DOI: 10.1080/08820538.2016.1228397]

22 **Lechner J**, O'Leary OE, Stitt AW. The pathology associated with diabetic retinopathy. *Vision Res* 2017; **139**: 7-14 [PMID: 28412095 DOI: 10.1016/j.visres.2017.04.003]

23 **Rajalakshmi R**, Prathiba V, Mohan V. Does tight control of systemic factors help in the management of diabetic retinopathy? *Indian J Ophthalmol* 2016; **64**: 62-68 [PMID: 26953026 DOI: 10.4103/0301-4738.178146]

24 **Danilova IG**, Sarapultsev PA, Medvedeva SU, Gette IF, Bulavintceva TS, Sarapultsev AP. Morphological restructuring of myocardium during the early phase of experimental diabetes mellitus. *Anat Rec* (Hoboken) 2015; **298**: 396-407 [PMID: 25251897 DOI: 10.1002/ar.23052]

25 **Radenković M**, Stojanović M, Prostran M. Experimental diabetes induced by alloxan and streptozotocin: The current state of the art. *J Pharmacol Toxicol Methods* 2016; **78**: 13-31 [PMID: 26596652 DOI: 10.1016/j.vascn.2015.11.004]

26 **Lenzen S**. The mechanisms of alloxan- and streptozotocin-induced diabetes. *Diabetologia* 2008; **51**: 216-226 [PMID: 18087688 DOI: 10.1007/s00125-007-0886-7]

27 **Szkudelski T**. The mechanism of alloxan and streptozotocin action in B cells of the rat pancreas. *Physiol Res* 2001; **50**: 537-546 [PMID: 11829314]

28 **Gelashvily OA**. Variant of periodization of biologically similar stages of human and rat`s ontogenesis (in Russian). *Saratov J Med Sci Res* 2008; **4**: 125-126

29 **Karpischev AI**. Medical laboratory technology (in Russian). St. Petersburg: Intermedika, 2002

30 **Yakovleva GE**. The enzymes in clinical biochemistry (in Russian). Novosibirsk: Vector-Best, 2005

31 **Jeppsson JO**, Kobold U, Barr J, Finke A, Hoelzel W, Hoshino T, Miedema K, Mosca A, Mauri P, Paroni R, Thienpont L, Umemoto M, Weykamp C; International Federation of Clinical Chemistry and Laboratory Medicine (IFCC). Approved IFCC reference method for the measurement of HbA1c in human blood. *Clin Chem Lab Med* 2002; **40**: 78-89 [PMID: 11916276 DOI: 10.1515/CCLM.2002.016]

32 **Kumar GL**, Rudbeck L. Education guide. Immunohistochemical (IHC) staining methods. California: Dako North America, Carpinteria, 2009: 224. Available from: URL: http://www.kanidis.gr/common/files/ANOSOISTOCHIMIA/DETECTION/ihc_staining_methods_5ed.pdf

33 **Taylor PR**, Martinez-Pomares L, Stacey M, Lin HH, Brown GD, Gordon S. Macrophage receptors and immune recognition. *Annu Rev Immunol* 2005; **23**: 901-944 [PMID: 15771589 DOI: 10.1146/annurev.immunol.23.021704.115816]

34 **Brochhausen C**, Schmitt VH, Mamilos A, Schmitt C, Planck CN, Rajab TK, Hierlemann H, Kirkpatrick CJ. Expression of CD68 positive macrophages in the use of different barrier materials to prevent peritoneal adhesions-an animal study. *J Mater Sci Mater Med* 2017; **28**: 15 [PMID: 27995493 DOI: 10.1007/s10856-016-5821-3]

35 **Weakley BS**. A beginner's handbook in biological transmission electron microscopy. Edinburg: Churchill Livingstone, 1981: 264

36 **Robinson R**, Barathi VA, Chaurasia SS, Wong TY, Kern TS. Update on animal models of diabetic retinopathy: from molecular approaches to mice and higher mammals. *Dis Model Mech* 2012; **5**: 444-456 [PMID: 22730475 DOI: 10.1242/dmm.009597]

37 **Capitão M**, Soares R. Angiogenesis and Inflammation Crosstalk in Diabetic Retinopathy. *J Cell Biochem* 2016; **117**: 2443-2453 [PMID: 27128219 DOI: 10.1002/jcb.25575]

38 **Park SH**, Park JW, Park SJ, Kim KY, Chung JW, Chun MH, Oh SJ. Apoptotic death of photoreceptors in the streptozotocin-induced diabetic rat retina. *Diabetologia* 2003; **46**: 1260-1268 [PMID: 12898017 DOI: 10.1007/s00125-003-1177-6]

39 **Nickla DL**, Wallman J. The multifunctional choroid. *Prog Retin Eye Res* 2010; **29**: 144-168 [PMID: 20044062 DOI: 10.1016/j.preteyeres.2009.12.002]

40 **Hua R**, Li Q, Wong IY, Ning H, Wang H. Choroidal microvascular proliferation secondary to diabetes mellitus. *Oncotarget* 2017; **8**: 2034-2036 [PMID: 28008140 DOI: 10.18632/oncotarget.14020]

41 **Melancia D**, Vicente A, Cunha JP, Abegão Pinto L, Ferreira J. Diabetic choroidopathy: a review of the current literature. *Graefes Arch Clin Exp Ophthalmol* 2016; **254**: 1453-1461 [PMID: 27109344 DOI: 10.1007/s00417-016-3360-8]

42 **Adini I**, Ghosh K, Adini A, Chi ZL, Yoshimura T, Benny O, Connor KM, Rogers MS, Bazinet L, Birsner AE, Bielenberg DR, D'Amato RJ. Melanocyte-secreted fibromodulin promotes an angiogenic microenvironment. *J Clin Invest* 2014; **124**: 425-436 [PMID: 24355922 DOI: 10.1172/JCI69404]

43 **Cherepanoff S**, McMenamin P, Gillies MC, Kettle E, Sarks SH. Bruch's membrane and choroidal macrophages in early and advanced age-related macular degeneration. *Br J Ophthalmol* 2010; **94**: 918-925 [PMID: 19965817 DOI: 10.1136/bjo.2009.165563]

44 **Aveleira CA**, Lin CM, Abcouwer SF, Ambrósio AF, Antonetti DA. TNF-α signals through PKCζ/NF-κB to alter the tight junction complex and increase retinal endothelial cell permeability. *Diabetes*

2010; **59**: 2872-2882 [PMID: 20693346 DOI: 10.2337/db09-1606]
45 **Nita M**, Grzybowski A, Ascaso FJ, Huerva V. Age-related macular degeneration in the aspect of chronic low-grade inflammation (pathophysiological parainflammation). *Mediators Inflamm* 2014; **2014**: 930671 [PMID: 25214719 DOI: 10.1155/2014/930671]
46 **Aizu Y**, Oyanagi K, Hu J, Nakagawa H. Degeneration of retinal neuronal processes and pigment epithelium in the early stage of the streptozotocin-diabetic rats. *Neuropathology* 2002; **22**: 161-170 [PMID: 12416555 DOI: 10.1046/j.1440-1789.2002.00439.x]
47 **Rizzolo LJ**. Barrier properties of cultured retinal pigment epithelium. *Exp Eye Res* 2014; **126**: 16-26 [PMID: 24731966 DOI: 10.1016/j.exer.2013.12.018]
48 **Grant WM**, Schuman JS. Toxicology of the Eye: Effects on the Eyes and Visual System from Chemicals, Drugs, Metals and Minerals, Plants, Toxins, and Venoms; Also, Systemic Side Effects from Eye med (4th edition). Springfield, Ill., USA: Charles C Thomas Pub Ltd., 1993: 1608
49 **Koskenoja M**. Alloxan diabetes in the pregnant mouse. Its effect on the offspring and particularly on their eyes. *Acta Ophthalmol Suppl* 1961; Suppl 68: 1-92 [PMID: 14458651]
50 **Emanuelli G**. Retinal ultrastructural alterations induced by alloxan in the rat (In Italian). *Rass Ital Ottalmol* 1964; **33**: 62-70

P- Reviewer: Das U, Koch TR **S- Editor**: Ji FF
L- Editor: A **E- Editor**: Song H

Published by **Baishideng Publishing Group Inc**
7901 Stoneridge Drive, Suite 501, Pleasanton, CA 94588, USA
Telephone: +1-925-223-8242
Fax: +1-925-223-8243
E-mail: bpgoffice@wjgnet.com
Help Desk: https://www.f6publishing.com/helpdesk
https://www.wjgnet.com